Silver Sintering Paste Rendering Low Porosity Joint for High Power Die Attach Application

Sihai Chen, Christine LaBarbera and Ning-Cheng Lee
Indium Corporation
Clinton, NY, 13323
schen@indium.com and nclee@indium.com

Abstract

Silver joints with ~10% porosity for die-attach have been achieved with specially engineered Ag sintering pastes, through combined pressureless sintering process plus thermal aging. The pastes developed in this work have the following advantages: 1) they can be used under pressure-less processing condition; 2) they are compatible with conventional reflow oven, resulting in a higher through-put as compared to that of stepwise heating oven; 3) they can be used under air reflow condition; 4) a highly reliable joint has been obtained as judged from the shear strength results from thermal aging and temperature cycling tests.

The silver sintering pastes are versatile in bonding different metallization surface including Au, Ag and Cu. It can also be used in bonding large area (10mm x 10mm) dies. Shear test results under varied temperatures implied that the maximum service temperature of Ag sintered joints can be as high as 470 – 530 °C, depending on the shear strength pass criteria, and this is more than 250°C higher than that of high-Pb joints.

Thermal aging test at 250°C for the joints generated on Ag-die/Au-DBC combination revealed that Ag continuously consolidates in the bulk phase resulting in the formation of larger pores with reduced numbers as compared to that of untreated samples. At the same time, it diffuses to sintered Ag/Au-DBC interface to form a dense Ag layer induced by alloying with Ni(Au) and Cu, which strengthened the bonding. A large bondline thickness is critical for obtaining highly reliable joints. The total porosity of the joint is found slightly decreased during the course of 3200h aging test. Temperature cycling at -55 ^{o}C to 200^{o}C shows that the silver joints are stable for at least 1000 cycles.

Key words: Silver sintering paste, die-attach, porosity, reliability, high temperature aging, temperature cycling

Introduction

Reliable and environmentally friendly interconnect materials used in high power and high temperature die- or substrate-attachment have attracted wide interest. At present, despite the highly toxic nature of lead (Pb), high Pb solder such as 92.5Pb5Sn2.5Ag and Pb5Sn is commonly used for 150 to 250°C applications. However, alternative materials that do not contain Pb is strongly desired, considering the global trend driven by the Restriction of Hazardous Substances (ROHS) directives. [1]

Sintered Ag is a very promising Pb-free candidate considering the following advantages: 1) it has a processing temperature similar to or even lower than that of current high-lead solders; 2) it has higher service temperature capabilities owing to its high melting point 961^{o}C; 3) it has higher value in thermal conductivity as compared to that of solder; 4) it has superior mechanical and electrical properties compared with other lead-free alternatives in the market. [2] A lot of research work has been conducted for power die attach, at first using process under pressure of 20 to 40 MPa, [3, 4] and then using the low pressure [5] or pressure-less process. [6,7]

For joints prepared by pressure-less sintering process, one concern about the silver sintering joint is the high porosity. Silver joint with 26% to 32% of porosity has been reported during 3000h of aging at 300°C. [8] In contrast, a value of 15% or even 3% can be achieved using pressure sintering process. [9] In this work, Ag joint with a low porosity of less than 10% or even 5% can be achieved under a pressureless sintering condition plus thermal treatment. Highly reliable silver joints using Ag-Si/Au-DBC combination have been confirmed through thermal aging at 250°C and thermal cycling (-55 to 200°C) tests. We observed that a large bondline thickness (BLT) plays a critical positive role in achieving the high reliability of the silver joints.

Experimental

Si die: the size of the Si die studied is 3mm x 3mm, 5mm x 5mm or 10mm x 10mm. The Au metallization is Ti/Ni/Au with 75nm/300nm/75nm thickness. The Ag metallization is Ti/Ni/Ag with 75nm/300nm/75nm thickness. For the test of Cu on direct bonded copper (DBC) surface, a 3mm x 3mm Cu block with 0.75mm thickness was used. DBC: The DBC size is 0.925" x 0.925"; ceramic thickness was 0.015", and Cu thickness was 0.012" on both sides. For the Au coated DBC, the coating is with Ni layer thickness of 3.5 µm and Au 200 nm. For the Ag coated DBC, the Ag thickness is 8 µm. Sample assemblies: a 4 mil stencil was used to print the paste on the DBC substrates, and pick and place machine was used to place the die on it.

Sintering condition: The pressure-less sintering was conducted through an IR reflow oven. Depending on the size of different die, different profiles are used. The typical sintering profile for sample C1 is shown in Figure 1.

Die shear test: After thermal aging or thermal cycling treatment, the die was tested for shear strength at ambient temperature using a XYZTEC Condor 250 shear tester. For testing samples C1 and high-Pb (92.5Pb5Sn2.5Ag) at elevated temperatures, a hot stage was used. The die was sheared at various temperatures up to 300°C to determine the maximum service temperature.

Morphology analysis: After the shear test, some samples were examined by optical microscopy for morphology, and were further cross-sectioned for microstructure analysis via scanning electron microscopy (SEM) and energy dispersive spectroscopy (EDS). As a control, some of the samples were cross-sectioned without running through the shear test.

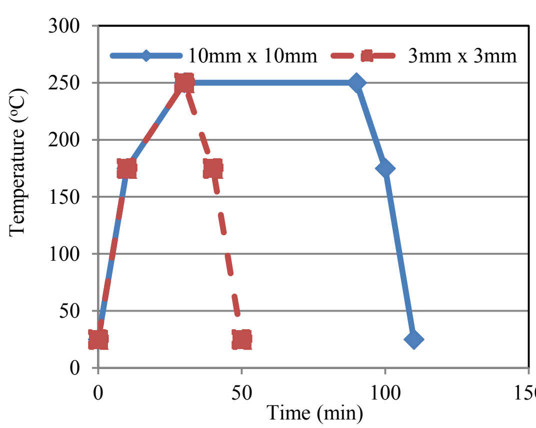

Figure 1. Sintering profiles of sample C1 for different sized dies.

Results and discussion

1. Samples after sintering

1.1 Effect of metallization

The metallization layer on Si/DBC pair plays a critical role for the joint strength because it determines the interface between sintered Ag and Si as well as DBC. As shown in Figure 2, on Au-DBC surface, die with Ag metallization shows higher shear strength of 64.62 MPa as compared to that of 44.22 MPa for die with Au metallization. Similar case is observed on Ag-DBC surface (Figure 2 red). The phenomenon that Au metallization shows a weaker shear strength has been reported before during 300°C aging test, and is normally attributed to the generation of "depletion layer". [8,10] It is interesting to see that the copper dies give strong shear strength on both Au-DBC and Ag-DBC surface at 54.84 MPa and 35.69 MPa, respectively, indicating that the paste is versatile in bonding to the copper material surface even without noble metal metallization.

1.2 Effect of die size

The shear strength of the joint generated on Ag-die/Au-DBC pair with different die sizes is shown in Figure 3. Normally, a longer heating profile is needed in order to well sinter the paste for larger sized dies (Figure 1). As the die size increases, lower shear strength is normally observed, presumably due to a higher internal stress. For the 5mm x 5mm die, shear strength of ~23MPa is observed. For the 10mm x 10mm die, due to the shear strength maximum limitation of the machine, the die still bond on the substrate after the test, indicating that the real shear strength of the joint is larger than the reading value of 11.2MPa.

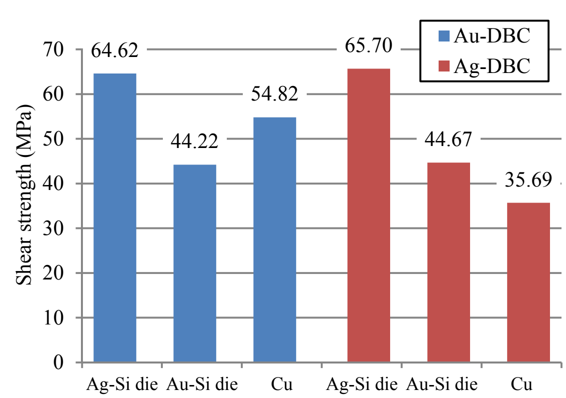

Figure 2. Shear strength of the Ag joints formed on Au-DBC (blue) and Ag-DBC surface (red) with Ag-, Au-coated die and Cu block. 3mm x 3mm die size, a heating profile with half hour longer than that in Figure 1 is used.

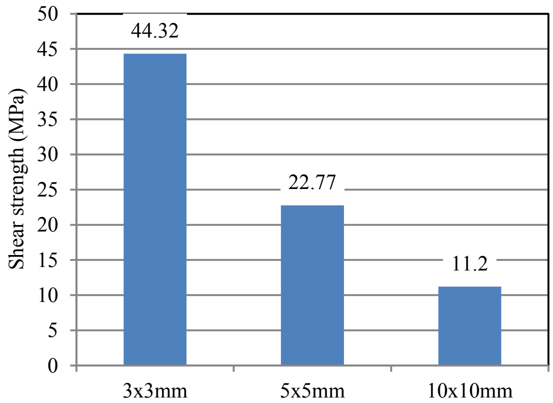

Figure 3. Shear strength of the Ag joints formed with different die sizes.

1.3 High temperature shear test

In order to compare the maximum working temperature between the Ag sintering paste and the high-Pb solder, the shear strength is measured under high temperature during shearing. The test results are shown in Figure 4. It is found that even at 300 ^oC, where high Pb solder melted, shear strength of the Ag joint can still reach 24MPa, demonstrated the high temperature capability of the silver sintering joints. According to the international standard IEC 60749-19: Semiconductor devices – Mechanical and climatic test methods – Part 19: Die shear strength, for a die area of 9 mm^2, the pass criteria is 15N or higher, which is 1.67 MPa. By extrapolation, the working temperature of silver sintered joint can be as high as 530 ^oC, almost 250 ^oC higher than that of the high Pb solder. If a stricter requirement of 6.1Mpa is used as pass criteria, maximum service temperature of Ag sintered joints can be as high as 470°C, versus 230°C for high-Pb joints.

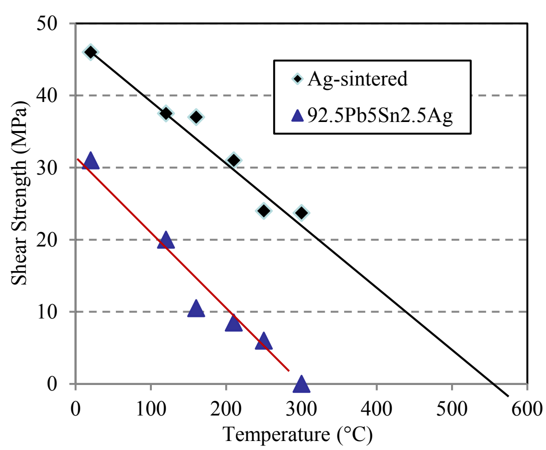

Figure 4. Shear strength of the Ag sintered and 92.5Pb5Sn2.5Ag joints obtained at different temperatures.

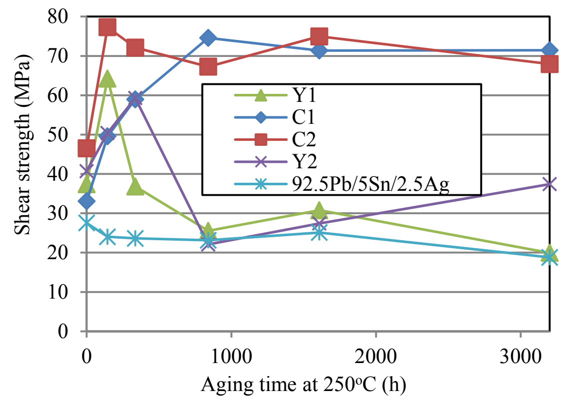

Figure 5. Shear strength of the Ag sintered and 92.5Pb5Sn2.5Ag joints after thermal storage at 250^{o}C for different times.

2. 250^{o}C thermal storage

2.1 Shear strength

Four Ag sintering pastes were evaluated, including C1 and C2 (C sintered at 250^{o}C and 280^{o}C peak temperature, respectively), Y1 and Y2. High Pb 92.5Pb/5Sn/2.5Ag solder paste (Type 3 powder size, 90% metal content) was used as a control. For all sintering pastes, a pressure-less sintering process was used, with a customized sintering profile for each paste. 3mm x 3mm dies in Ag-Si/Au-DBC combination are used in this experiment.

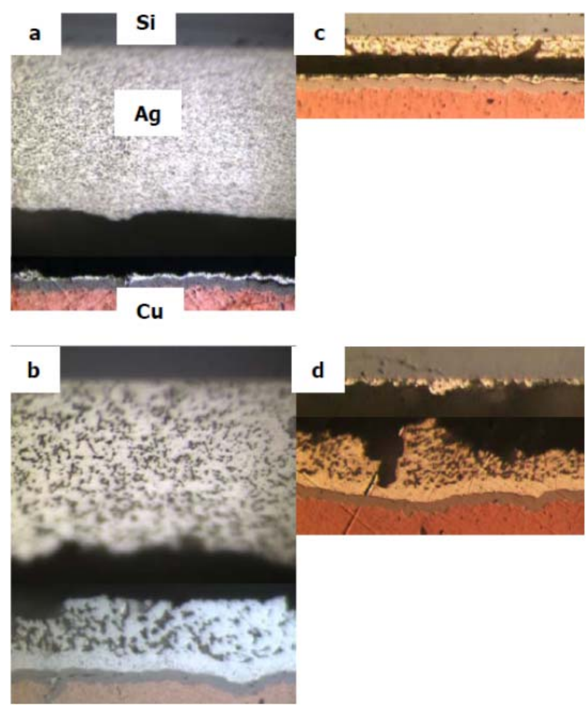

Figure 6. Optical microscopic images showing the failure point of the sheared samples for C1 before (a) and after (b), and Y2 before (c) and after (d) 336h of 250^{o}C aging, respectively.

In the initial stage of thermal storage at 250°C, such as at 144h, all the Ag sintered joints show an increase in shear strength (Figure 5). After further aging, a drastic decrease in shear strength was observed for Y1 and Y2 (from 336h). In contrast, the shear strength of C1 further increased and then leveled at around 70MPa until 3200h. For sample C2, the shear strength kept in the range of 68 to 78Mpa until 3200h. In order to understand the cause of the above difference, the sheared samples are cross-sectioned and two examples for samples C1 and Y2 are shown in Figure 6. One observation is that before thermal aging, the failure location is normally near the DBC side of the joint (Figure 6 a and c). After 336h of aging, the interface at DBC side is apparently

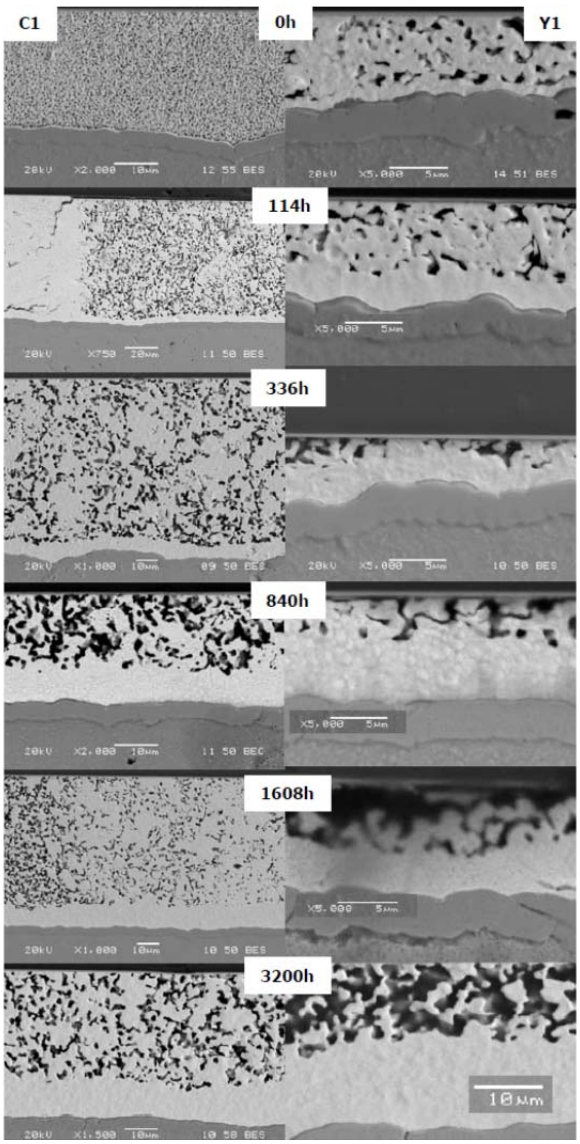

Figure 7. SEM images showing the development of the silver sintering joints for samples C1 and Y1 under 250°C aging.

strengthened by the formation of a thick dense layer. The failure location has moved away from the DBC side to the sintered Ag bulk phase (Figure 6c) or near the Si side (Figure 6d). Bondline thickness shows great impact in these two cases, for sample C1 having a thick BLT, the joint is more robust against thermal aging, while a thin BLT results in a weak joint during aging for sample Y2. Samples C1 and C2 have BLT in the range of 25 to 80 µm, samples Y1 and Y2 in the range from 5 to 25 µm.

For the high-Pb samples, the shear strength decreased 32% in intensity after 3200h of aging, and we observed the generation of voids and cracks in the Si die/ solder interface.

2.2 Dense layer formation

To further understand the change of Ag sintered joint during aging, cross-section was conducted for all the samples. Examples for samples C1 and Y1 are shown in Figure 7. One can see that a dense layer is built up on DBC side and increases in thickness continuously as the aging proceeds for both samples. A quantitative measurement of the thickness change for all the samples is shown in Figure 8. In the initial 114h of aging, the average growth rates are calculated as 28.2, 32.7, 11.3 and 21.3nm/h for samples C1, C2, Y1 and Y2, respectively. These rates are much higher than that of the average growth rate in the whole 3200h aging time, which are 3.2, 2.7, 3.3, and 4.1nm/h for sample C1, C2, Y1 and Y2, respectively. That means, the dense layer is built up quickly in the initial stage of aging. Also, it is noticed in Figure 8 that a higher growth rate is seen for sample with a larger BLT in the initial stage of aging (C1 and C2 vs Y1 and Y2). For the thin BLT samples Y1 and Y2, after 3200h of aging, the dense layer thickness is 13 and 16 µm, respectively. These numbers account for 55% and 88% of the BLT (see

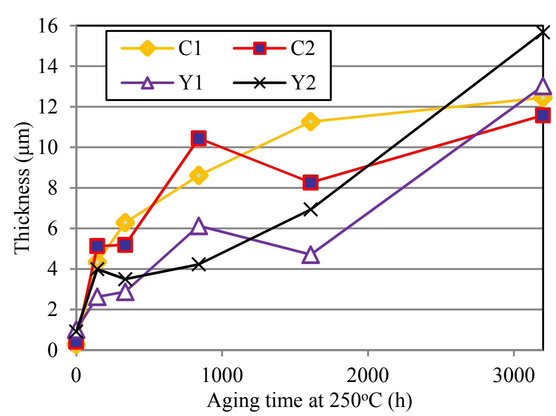

Figure 8. Growth of BLT during thermal aging for samples C1, C2, Y1 and Y2.

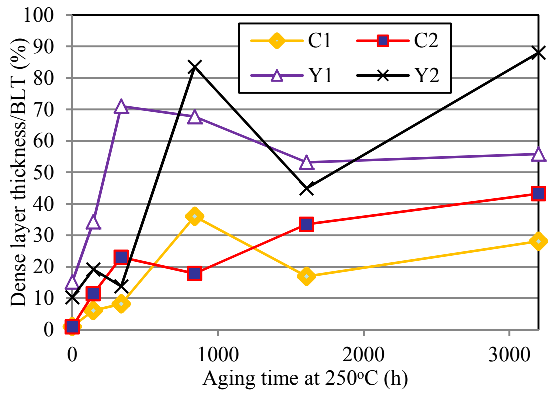

Figure 9. Dense layer thickness/BLT during thermal aging for samples C1, C2, Y1 and Y2.

Figure 9). As shown in Figure 7, for sample Y1, after long time of aging (336h, 840h, 1608h and 3200h), very large pore or void are generated in the bulk phase, which is apparently the weakest spot during shear test. The formation of this structure is caused by Ag diffusion away from bulk phase toward DBC side to form the dense layer.

2.3 Dense layer composition

As shown in Figure 7, a dense layer formation combined with a large BLT will help avoiding the generation of large porous structure in bulk phase (sample C1), and thus increasing the thermal aging reliability. Why a dense layer is generated for all the silver sintered samples? Elemental analysis was conducted to answer this question. As shown in Figure 10a areas 4, 3 and 2 for sample Y1, the atomic composition of the dense layer near the DBC side has been characterized as 91Ag/2.2Cu/4.8Ni/2Au, 95.6Ag/2Cu/2.4Ni, and 94.7Ag/1.8Cu/2.1Ni, respectively. In the area 1 near the Si die side, the composition is 3.2Si/2.7Ni/94.1Ag. This shows that tendency for Ag to migrate to the DBC to form a dense layer is driven by the tendency for Ag to alloy with Ni, Cu, and Au. The supply of Ni and Cu is plenty on the DBC side; while that on the die side is very limited due to the thin layer of Ni on die. Note that there is no pure Ag area in the joint after 840h of aging.

For the sample C2 with a larger BLT, 100% pure Ag area was detected in the center of the joint (Figure 10b areas 2 and 3), indicating that there are plenty of supply of silver in the bulk phase to mitigate the loss caused by Ag diffusion, thus help maintaining the integrity of the joint after long time of aging.

The dense layer composition was studied for all the samples, an example was shown in Figure 11 for

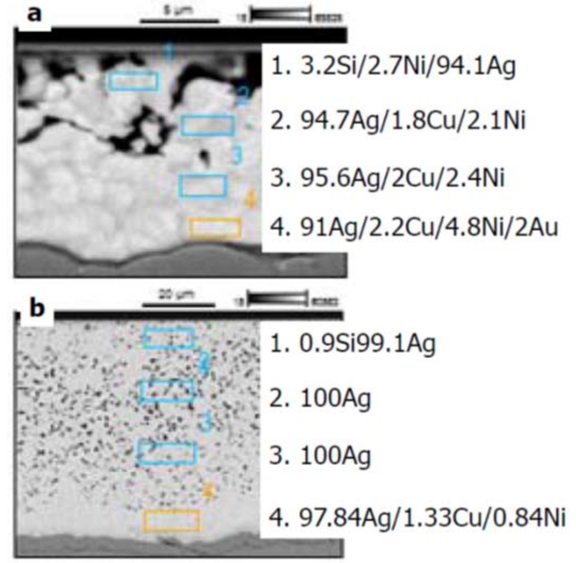

Figure 10. Composition analysis results at different locations within the joint for samples a) Y1 and b) C2 aged for 840h at 250°C.

sample C1. Before thermal aging, a high amount of Ni (37%) was detected, this may not reflect the dense layer composition, because the thickness is very thin at this time, and is difficult to be detected due to the EDX probe area limitation. After the aging, we continuously detect about 1% to 5% of Ni even after 3200h. Cu is also constantly detected in the range of 1% to 5% during the aging process. Au is detected in some samples at different aging times, but not always. This confirms that the elements of dense layer are AgNiCuAu, with a quantitative composition estimated as $Ag_{85\text{-}98}Ni_{1\text{-}5}Cu_{1\text{-}5}Au_{0\text{-}5}$.

2.4 Shear failure site at time zero on aging

For a sintered Ag joint, the failure site occurred at interface between sintered Ag layer and DBC when

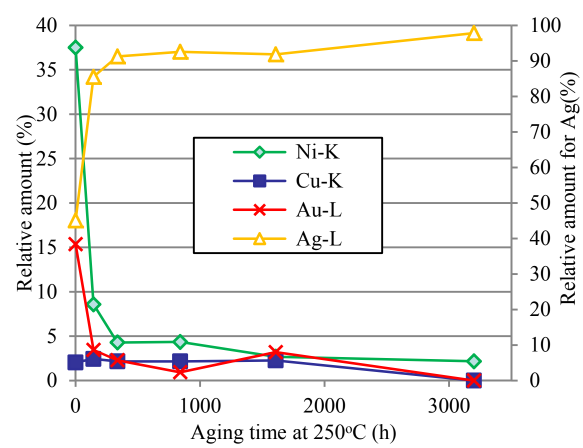

Figure 11. Composition analysis results for the dense layer in sample C1 aged at different time at 250°C.

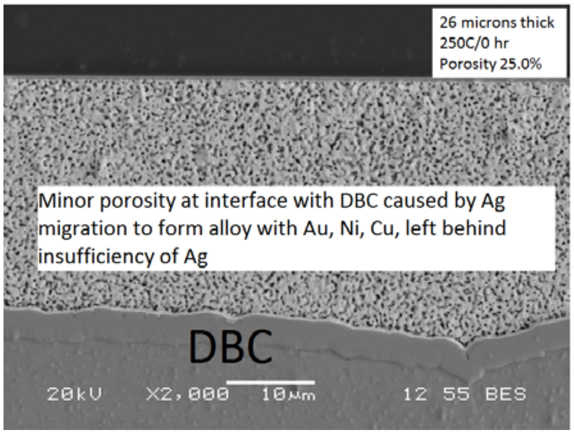

Figure 12. SEM image of sample C1 at time zero of aging treatment, with a thin layer of Ag on top of DBC, and a narrow concentrated porosity layer on top of the thin Ag layer.

conducting die shear test. Careful scrutiny revealed that a silver layer has already generated on DBC surface, as exemplified by Figure 6(a) for C1 and 6(c) for Y2. Figure 12 shows the close up look of C1 sample at time zero of thermal aging after sintering at 250°C. A very thin solid Ag layer can be recognized on top of DBC. Above that is a concentrated small porosity layer. At sintering, Ag migrated toward DBC and formed a 0.5 μ dense Ag layer due to alloying, and the concentrated porosity layer resulted from loss of Ag. The latter explained the site of failure when conducting die shear test. This concentrated porosity layer gradually vanished through continuous Ag migration upon further 250°C aging, and the shear failure site moved away from the interface accordingly.

2.5 Total porosity

By comparing the cross-section images of the aged C1 samples to that of the un-aged one (Figure 7), pore size of the joint increased drastically from 500nm to around 1 μm, showing that silver sintering

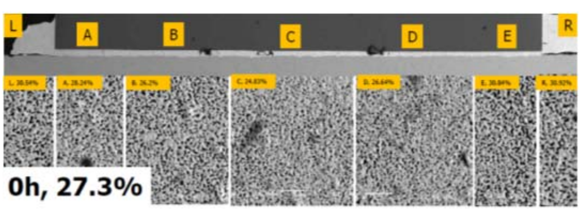

Figure 13. Total porosity of sample C1 before thermal aging. SEM of 5 zones under the joint area is measured and total porosity is calculated. Similar method is used for calculating total porosity of aged samples (not shown).

or migration occurred continuously in the bulk phase. This will definitely result in the change in porosity. It

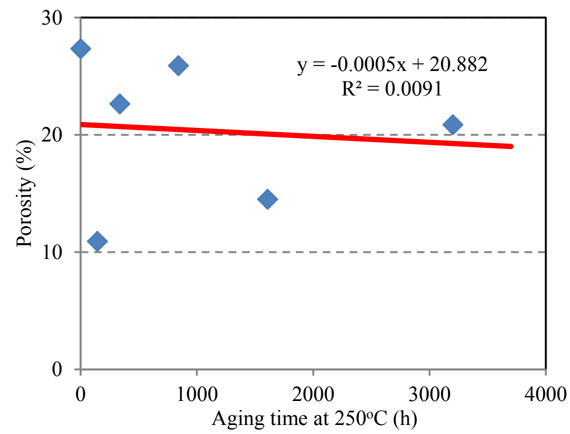

Figure 14. Total porosity of sample C1 during aging with bondline thickness uncontrolled.

will be interesting to know how the total porosity changes during aging.

To measure the total porosity, SEM images of the whole joint were taken at 5 different locations, as shown in Figure 13 locations A – E. The porosity of each area was then measured using image analysis software. Combined with the data of area percentage of different locations, the total porosity can then be obtained. As shown in Figure 14, overall, the total porosity during aging for samples C1 decreased slightly with increased thermal aging time. This implies that these Ag joints are very stable under aging.

Since the BLT of samples prepared under different aging conditions is not strictly kept the same, the data

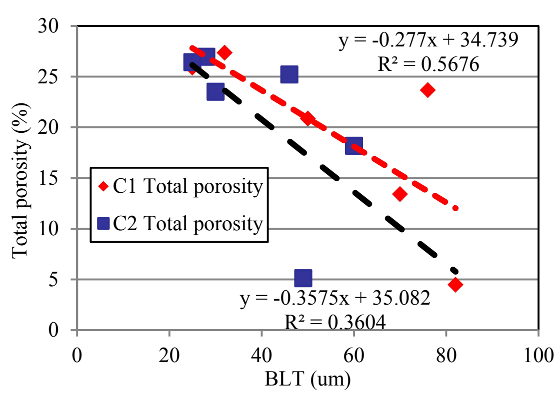

Figure 15. Total porosity vs BLT for samples C1 and C2 at different aging times.

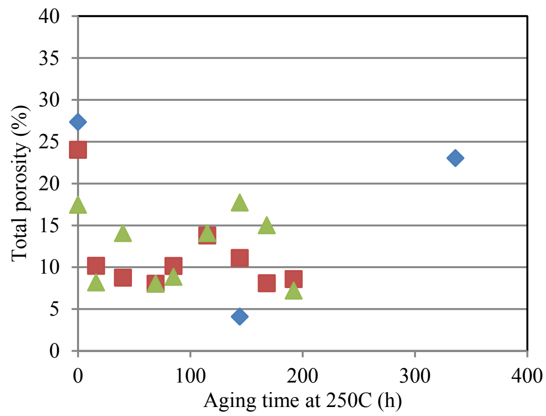

Figure 16. Total porosity vs aging time at 250^{o}C. Diamond, triangle and square symbols represent experimental data with different batch of tests.

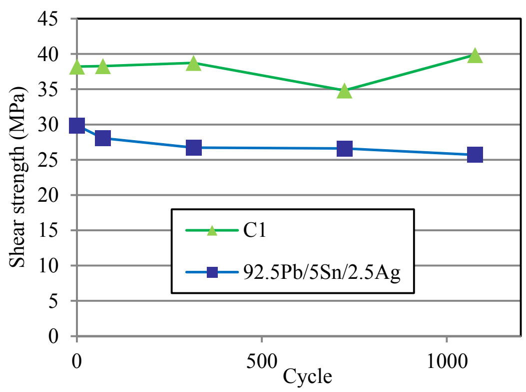

Figure 17. Shear strength of the Ag sintered and 92.5Pb5Sn2.5Ag joints obtained at different TCT cycles.

points between total porosity and BLT of each sample are plotted regardless of the aging time. As shown in Figure 15, a strong relation was observed for both samples C1 and C2 that total porosity decreased as the BLT increased.

2.6 ~10% Total porosity

As shown in Figure 14, after 144h of aging, a very low total porosity of ~10% has been obtained. Further detailed study has been conducted by aging the sintered samples at 250^{o}C for shorter times; the total porosity measured is shown in Figure 16. A quick decrease in total porosity from around 25% to 10% was observed within 16 h of aging and the porosity kept almost at around 10% under less than 100h of aging. These experiments confirmed that very low porosity can be obtained under pressureless treatment conditions.

3. Thermal cycling test

Shear strength of samples C1 and high Pb before and at different -55 ^{o}C to 200^{o}C thermal cycles is displayed in Figure 17. The high Pb joint decreased 14% in intensity after 1076 cycles, while that of Ag joint kept at 35 to 40Mpa during the test period, demonstrating the robustness of the silver joint. Test is not continued over 1076 cycles due to the formation of cracks in the DBC substrates. Figure 18 gives the SEM image of the Ag joint before and after thermal cycling. Before cycling, similar porous structure was observed all over the joint; after thermal cycling, low porosity zone was formed in the center area, while porous structure is observed at both end of the joint area. As the number of cycle increased, the pore size of the end zones increased, however, the total porosity did not increase.

Discussion

The formation of the center dense end porous structure has been observed in both thermal aging and cycling tests. However, this structure is not observed in the as-sintered samples (Figures 13 and

Figure 18. SEM image of the C1 Ag joints obtained at different TCT cycles.

18). This shows that heat supply will accelerate continuous sintering, especially in the center part of the joints. The formation of the above structures has been observed before, and is linked to the original placement process, due to the tendency for the particulates to flow out of the gap at a slightly reduced velocity compared to the liquid component of the paste. [10] We tend to regard this factor as minor because the as-sintered samples give a very even distribution of the pore in the whole joint, with a slightly difference in porosity between end and center areas (28.2% vs 24.8%). The drastically reduced center porosity may be due to the continuous sintering assisted by the residue solvent in the center area, while the porous structure at the end is inevitable as the solvent evaporation channels. The solvent residue in the center area is often observed when a large area of die is used and the sintering heating profile is not long enough.

Continuous densification in the bulk phase of the joint is based on atomic diffusion driven by the reduction of interfacial energy. Possible diffusion routes for a two particle sintering model includes non-densification and non-shrinkage Paths 1 and 2 corresponding to surface and lattice diffusion, respectively. In the later stage of the sintering, densification occurred through Through-Lattice Diffusion (Path 3) and Grain Boundary Diffusion (Path 4). [11] In Paths 3 and 4, the centers of spherical particles approach one another, and the neck between them widens, increasing the particle contact area. The formation of the dense structure can be attributed to these processes. As results, fewer pores are observed instead.

Comparing the shear strength of the sample C1 in thermal aging to that in thermal cycling, the former can reach ~70Mpa after 840h of aging, while the latter only kept at ~40MPa. A much thicker silver dense layer is observed in the former case. Apparently, silver atom diffusion to the DBC side to alloy with Cu and Ni (Au) plays a critical role in strengthening the joint. The "alloying" behavior has been previously discussed in the cases where a thick layer of Au (~2 μm [10] or ~10 μm [8] in thickness) on ceramic substrate is applied. Interdiffusion between Ag and Au has been observed. In those cases, a high porosity zone or a so-called "depletion zone" is generated adjacent to the dense layer, Ag diffuses through the grain boundaries or pore inner surface of the bulk phase to the exposed Au creating a continuous dense layer. The "consumption" of Ag from bulk phase generates the depletion layer, resulting in Kirkendall voids. [8,10] Interestingly, we show that a large BLT and/or better paste chemistry can effectively repair/avoid this void formation.

Conclusion

The silver sintering pastes are versatile in bonding different metallization surface including Au, Ag and Cu. It can also be used in bonding large area (10mm x 10mm) dies. Shear test results under varied temperatures implied that the maximum service temperature of Ag sintered joints can be as high as 470 – 530 °C, depending on the shear strength failure criteria, and this is more than 250°C higher than that of high-Pb joints.

Thermal aging test at 250°C for the joints generated on Ag-die/Au-DBC combination revealed that Ag continuously consolidates in the bulk phase through generating larger aggregates and pore with reduced numbers. In the same time, it diffuses to the sintered Ag/Au-DBC interface to form a dense Ag layer by alloying with Cu and Ni(Au), strengthening the bonding. A large bondline thickness is critical for obtaining highly reliable joints.

Temperature cycling at -55 ^{o}C to 200^{o}C shows that the silver joints are stable for at least 1000 cycles.

Acknowledgements

The authors are grateful to Snow Yan for preparation of samples Y1 and Y2.

References

[1] K. Suganuma, S.J. Kim, and K.S. Kim, "High-Temperature Pb-Free Solders: Properties and Possibilities" JOM 61, 64 -65, 2009.

[2] V.R. Manikam and K.Y. Cheong, "Die Attach Materials for High Temperature Applications: A Review" IEEE Trans. Compon. Packag. Manuf. Technol. 1, 457 – 478, 2011.

[3] H. Schwarzbauer, "Method of Securing Electronic Components to a Substrate," U.S. Patent 4810672, Mar. 1989.

[4] C. Gobl and J. Faltenbacher, "Low Temperature Sinter Technology Die Attachment for Power Electronic Applications," in Proc. 6th Int. Conf. Intergr. Power Elctron. Syst., Nuremburg, Germany, 1-5, 2010.

[5] H. Zheng, D. Berry, J. N. Calata, K. D. T. Ngo, S. Luo, and G-Q Lu, "Low-Pressure Joining of Large-Area Devices on Copper Using Nanosilver Paste", Components, Packaging and Manufacturing Technology, IEEE Transactions on 3.6, 915-922, 2013.

[6] J. G. Bai, and G-Q Lu, "Thermomechanical Reliability of Low-Temperature Sintered Silver Die Attached SiC Power Device Assembly", Device and Materials Reliability, IEEE Transactions on 6.3, 436-441, 2006.

[7] Tao Wang, Meihua Zhao, Xu Chen, Guo-Quan Lu, Khai Ngo, Shufang Luo, "Shrinkage and Sintering Behavior of a Low-Temperature Sinterable Nanosilver Die-Attach Paste", J. Electron Materials, Vol. 41, No. 9, 2543-2552, 2012.

[8] F. Yu, R. W. Johnson, and M. Hamilton, "Pressureless, Low Temperature Sintering of Micro-Scale Silver Paste for Die Attach for 300^{o}C Applications" IMAPS Conference & Exhibition on HiTEN 2014, May 13-15, 165-171, 2014.

[9] Thomas Herboth, Michael Guenther, Andreas Fix, Juergen Wilde, "Failure Mechanisms of Sintered Silver Interconnections for Power Electronic Applications", 2013 Electronic Components & Technology Conference, 1621 – 1627, 2013.

[10] G. Lewis, G. Dumas, S. H. Mannan, "Evaluation of Pressure Free Nanoparticle Sintered Silver Die Attach on Silver and Gold Surface" IMAPS Conference & Exhibition on HiTEN 2013, July 8-10, 237-245, 2013.

[11] J. Frenkel, "Viscous Flow of Crystalline Bodies under the Action of Surface Tension" J Phys (USSR) 9, 385-391, 1945.